

Studies of multiple stellar systems – III. Modulation of orbital elements in the triple-lined system HD 109648

Saurabh Jha,¹ Guillermo Torres,¹ Robert P. Stefanik,¹ David W. Latham¹
and Tsevi Mazeh² \star

¹*Harvard-Smithsonian Center for Astrophysics, 60 Garden Street, Cambridge, MA 02138, USA*

²*School of Physics and Astronomy, Raymond and Beverly Sackler Faculty of Exact Sciences, Tel Aviv University, Tel Aviv, Israel*

submitted September 22, 1999; accepted March 30, 2000

ABSTRACT

The triple-lined spectroscopic triple system HD 109648 has one of the shortest periods known for the outer orbit in a late-type triple, 120.5 days, and the ratio between the periods of the outer and inner orbits is small, 22:1. With such extreme values, this system should show orbital element variations over a timescale of about a decade. We have monitored the radial velocities of HD 109648 with the CfA Digital Speedometers for eight years, and have found evidence for modulation of some orbital elements. While we see no definite evidence for modulation of the inner binary eccentricity, we clearly observe variations in the inner and outer longitudes of periastron, as well as in the radial velocity amplitudes of the three components. The observational results, combined with numerical simulations, allow us to put constraints on the orientation of the orbits.

Key words: celestial mechanics, stellar dynamics – binaries: spectroscopic – stars: individual: HD109648.

1 INTRODUCTION

The number of triple systems with well-determined orbital elements is still small (Fekel 1981; Tokovinin 1997, 1999). In particular, the number of spectroscopic triples in which the wide orbit is also known from radial-velocity observations is very small. Part of the problem is that the velocity amplitude of the outer binary is usually small compared to the amplitude of the inner binary. Moreover, after a binary orbit has been solved, the natural reaction is to discontinue observing it, and checks for longer-term variations are rarely made (Mayor & Mazeh 1987). This series of papers is aimed at increasing our knowledge of triples by investigating systems where the inner and outer orbits can both be determined from spectroscopic observations. The first paper of the series (Mazeh, Krymolowski and Latham 1993, hereinafter Paper I) examined the halo triple G38-13, while the second paper (Krymolowski and Mazeh 1998, hereinafter Paper II) derived an analytic technique which allows for fast simulation of orbital modulations of a binary induced by a third star.

In the present paper we analyse the triple-lined spectroscopic triple system HD 109648 (HIP 61497, $\alpha =$

$12^{\text{h}}35^{\text{m}}59^{\text{s}}.8$, $\delta = +36^{\circ}15'30''$ (J2000); $V = 8.8$). HD 109648 was identified as one (star 6) of a handful of stars belonging to the remnant of a nearby old open cluster, Uppgren 1 (Uppgren & Rubin 1965), but subsequent studies have weakened the interpretation that all of the stars originally identified are physically associated (Uppgren, Philip & Beavers 1982; Gatewood et al. 1992; Stefanik et al. 1997; Baumgardt 1998).

The triple-lined nature of HD 109648 was noticed soon after we began observing it, because the one-dimensional correlations of some of the spectra clearly showed three peaks. A periodicity analysis revealed periods at ~ 5.5 and ~ 120 days. Triple systems tend to be hierarchical, usually with a close binary and a more distant third star, as other configurations are generally unstable and are unlikely to persist and be detected. To first-order, a hierarchical triple system can be separated into an inner orbit (comprising the two close stars) and an outer orbit (comprising the third star and the centre-of-mass of the inner pair). This approximation is most valid when the distance to the third star far exceeds the separation between the inner two stars. One of the goals of this study is to investigate the interaction of these three stars (through the variation of the inner and outer orbits) to higher order.

A preliminary version of this work was presented at a conference entitled ‘Thirty Years of Astronomy at the Van Vleck Observatory: A Meeting in Honor of Arthur R. Up-

\star E-mail: {sjha, gtorres, rstefanik, dlatham}@cfa.harvard.edu; mazeh@wise.tau.ac.il

gren’ (Jha et al. 1997). This paper updates the orbital solutions presented there and adds a significantly more detailed analysis of the system, partly through the use of numerical simulations.

In Section 2 we summarise the analysis of the observations, including the derivation of the radial velocities, orbital solutions, and additional parameters such as the mass ratios and constraints on the orbital inclinations. We discuss the theoretically expected modulations of orbital elements in Section 3. In Section 4 we describe our efforts to search for such variations and present our results. Further constraints for the system via numerical simulation are derived in Section 5. Finally, in Section 6 we discuss our results and relate them to previous and future work.

2 RADIAL VELOCITIES AND ORBITAL SOLUTIONS

HD 109648 has been monitored since 1990 with the Center for Astrophysics (CfA) Digital Speedometer (Latham 1985; Latham 1992) on the 1.5-m Wyeth Reflector at the Oak Ridge Observatory, located in the town of Harvard, Massachusetts. The echelle spectra cover 45 Å centered at 5187 Å, with a spectral resolution of $\lambda/\Delta\lambda \approx 35,000$. As of 1998, we have secured 290 spectra of HD109648.

Radial velocities were derived for each of the three stars in the system using the three-dimensional version (Zucker, Torres & Mazeh 1995) of the two-dimensional correlation technique TODCOR (Zucker & Mazeh 1994). TODCOR assumes that the spectrum for each individual star in the system is known, and that an observed spectrum is composed of the individual component spectra added together, each shifted by its own radial velocity. Thus, to use TODCOR successfully one must have suitable template spectra for each of the components. We chose our templates from a grid of synthetic spectra calculated by Jon Morse using the 1992 Kurucz model atmospheres (e.g. Nordström et al. 1994).

Our first guess for the template parameters was based on a visual inspection of the spectra. Application of TODCOR yielded preliminary velocities for each of the three components, from which we determined the makeup of the triple: the inner binary consists of the primary and the tertiary, while the outer star is second in brightness. With this information, we were able to refine our templates to obtain the final velocities. For the primary we adopted an effective temperature, $T_{\text{eff}} = 6750$ K; solar metallicity, $[\text{m}/\text{H}] = 0$; and main-sequence surface gravity, $\log g = 4.5$ (cgs units). The period of the inner binary is quite short, and we assumed this has led to spin-orbit synchronization for the inner stars (see for example Mazeh & Shaham 1979). Therefore we adopted a rotational velocity of $v \sin i = 10$ km s⁻¹ for both of the inner binary stars. For the secondary and the tertiary, we have used a slightly cooler temperature, $T_{\text{eff}} = 6500$ K, and for the outer star we assumed that the rotation was negligible, $v \sin i = 0$ km s⁻¹. Small changes in the choice of template parameters did not have much effect on the radial velocities or orbital solutions. The final template parameters are listed in Table 1, and the individual radial velocities are reported in the Appendix.

For a proper solution of the orbital elements, one must

Table 1. Parameters for the synthetic template spectra.

Star	T_{eff} K	$\log g$ $\log(\text{cm s}^{-2})$	$[\text{m}/\text{H}]$ dex	v_{rot} km s ⁻¹
primary (Aa)	6750	4.5	0.0	10
secondary (B)	6500	4.5	0.0	0
tertiary (Ab)	6500	4.5	0.0	10

Table 2. HD 109648 mean orbital solution.

P_A	5.4784499 ± 0.0000080	days
K_{Aa}	62.02 ± 0.11	km s ⁻¹
K_{Ab}	68.98 ± 0.16	km s ⁻¹
e_A	0.0119 ± 0.0014	
ω_A	37.2 ± 7.1	deg
T_A	2448462.24 ± 0.11	HJD
$a_{Aa} \sin i_A$	4.6721 ± 0.0084	Gm
$a_{Ab} \sin i_A$	5.1965 ± 0.0122	Gm
$m_{Aa} \sin^3 i_A$	0.6719 ± 0.0034	M_{\odot}
$m_{Ab} \sin^3 i_A$	0.6041 ± 0.0026	M_{\odot}
P_{AB}	120.5275 ± 0.0080	days
K_A	17.20 ± 0.10	km s ⁻¹
K_B	34.91 ± 0.15	km s ⁻¹
e_{AB}	0.2362 ± 0.0033	
ω_{AB}	331.79 ± 0.84	deg
T_{AB}	2448412.19 ± 0.28	HJD
$a_A \sin i_{AB}$	27.70 ± 0.15	Gm
$a_B \sin i_{AB}$	56.23 ± 0.24	Gm
$m_A \sin^3 i_{AB}$	1.0862 ± 0.0114	M_{\odot}
$m_B \sin^3 i_{AB}$	0.5352 ± 0.0058	M_{\odot}
γ	-18.900 ± 0.055	km s ⁻¹
$\sigma(O - C)_{Aa}$	1.36	km s ⁻¹
$\sigma(O - C)_{Ab}$	1.97	km s ⁻¹
$\sigma(O - C)_B$	1.72	km s ⁻¹

solve for the inner and outer motions simultaneously. For this purpose we have used ORB20, a code developed at Tel Aviv University (Paper I), and a new code developed at the CfA. These two independent codes yielded the same results. Throughout this paper we employ the following notation for the elements of this hierarchical triple system. We label the inner stars Aa and Ab (with Aa being the brighter), while the centre-of-mass of the inner stars is denoted as A and the outer star is denoted B. When we are discussing orbits rather than the stars themselves, we designate the inner orbit as A and the outer orbit as AB.

The orbital solution using all 290 of our observations is displayed in Figure 1. The top panel shows the motion of the two inner stars, after their centre-of-mass motion has been removed. The bottom panel shows the centre-of-mass motion of the inner binary, as well as the motion of the third star. The derived average orbital elements of the inner and outer motions, as well as the overall radial velocity of the system, γ , are listed in Table 2.

The triple-lined nature of the spectra yields much more information about the system than can be gathered when only one component is visible (as was the case for G38-13 in Paper I). We can, for instance, determine the mass ra-

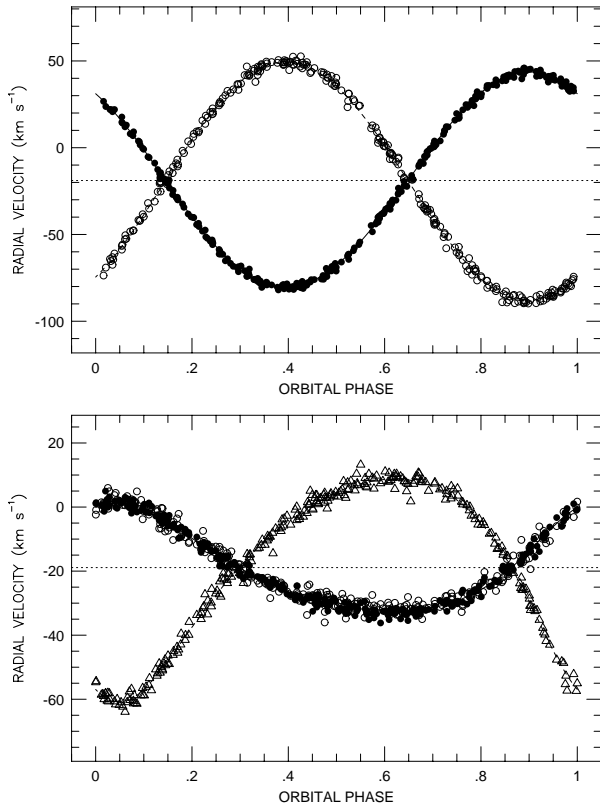


Figure 1. Simultaneous orbital solution for HD 109648 using all of the 290 observations. The upper panel shows the stars of the inner binary, Aa (filled circles) and Ab (empty circles), with their centre-of-mass motion removed. The lower panel shows the outer binary, comprised of the outer star B (triangles), as well as the common centre-of-mass motion of the inner stars. The observations have velocity residuals $\sigma_{Aa} = 1.36$, $\sigma_{Ab} = 1.97$ and $\sigma_B = 1.72$ km s⁻¹, part of which arises from the fact the orbital elements are not static.

tios between the three stars. The mass ratio of the inner pair is easily determined from the inner orbital elements, $m_{Aa}K_{Aa} = m_{Ab}K_{Ab}$. This results in

$$\frac{m_{Ab}}{m_{Aa}} = 0.8991 \pm 0.0027. \quad (1)$$

The same relation holds for the outer orbit, $m_A K_A = m_B K_B$, but in this triple system we know that $m_A = m_{Aa} + m_{Ab}$. Thus we derive

$$\frac{m_B}{m_{Aa}} = \frac{K_A}{K_B} \left(1 + \frac{K_{Aa}}{K_{Ab}} \right) = 0.9356 \pm 0.0072. \quad (2)$$

From the orbital elements and Kepler’s Third Law we can also derive the quantities $m_{Aa} \sin^3 i_A$ and $m_B \sin^3 i_{AB}$ (e.g., Batten 1973) listed in Table 2, which with the mass ratio lead to a ratio involving the inclination angles,

$$\frac{\sin i_{AB}}{\sin i_A} = 0.9478 \pm 0.0045. \quad (3)$$

The individual inclination angles remain unknown, and consequently, so do the exact masses of the stars, but we can estimate the masses by assuming the stars are still on the main sequence. Uppgren & Rubin (1965) report an MK spectral type of F6V for HD 109648. The light of the primary

dominates the spectrum of the system, so this spectral type corresponds to a primary mass (Gray 1992) of

$$m_{Aa} = 1.3 \pm 0.1 M_{\odot}, \quad (4)$$

where we have assumed solar metallicity and have adopted an uncertainty that corresponds to the spectral-type range F3V to F8V. Using the known mass ratios, we can then calculate the masses of the other two stars.

From the masses we can nearly determine the inclination angles. Since radial velocity measurements do not reveal the direction of orbital motion, we are left with an ambiguity between the following supplementary possibilities for each angle,

$$i_A = 53.4 \pm 2.0^{\circ} \quad \text{or} \quad 126.6 \pm 2.0^{\circ} \quad \text{and} \quad (5)$$

$$i_{AB} = 49.5 \pm 1.8^{\circ} \quad \text{or} \quad 130.5 \pm 1.8^{\circ}. \quad (6)$$

However, even if we were to resolve the ambiguities in the inclinations, we would still not know the complete geometric orientation of the system. Spectroscopic observations (as opposed to visual ones) do not provide the elements Ω_A and Ω_{AB} , the position angles of the inner and outer lines of nodes. Without these angles, we cannot determine an important quantity in the interaction of the two binaries—the relative inclination ϕ . The relative inclination is defined as the angle between the two orbital planes, or identically, the angle between the inner and outer angular momentum vectors. It is related to the individual inclination angles, and the angles of the lines of nodes, by (Batten 1973; Fekel 1981)

$$\cos \phi = \cos i_A \cos i_{AB} + \sin i_A \sin i_{AB} \cos(\Omega_A - \Omega_{AB}). \quad (7)$$

Since the quantity $\Omega_A - \Omega_{AB}$ is unknown, we can only limit its cosine between +1 and -1, resulting in a geometrical constraint on ϕ ,

$$i_A - i_{AB} \leq \phi \leq i_A + i_{AB}. \quad (8)$$

Nevertheless, from this result we can derive an important parameter, namely the minimum relative inclination angle, to see if the system can be coplanar. We determine that the minimum angle between the orbital planes is $\phi_{\min} = 3.9 \pm 0.3^{\circ}$. Thus the two orbits could be very close to coplanarity, but cannot be exactly coplanar. In Section 4 we strengthen this lower limit slightly.

3 EXPECTED EFFECTS OF THE THREE-BODY INTERACTION

As discussed in Papers I and II, the separation of the motions of a hierarchical triple system into inner and outer orbits is only a first-order approximation. The gravitational attraction of the outer body exerted on each of the two inner bodies is different from the gravitational attraction exerted on an imaginary body at the centre-of-mass of the inner binary system. The difference induces long-term modulations of some of the orbital elements of the system.

The timescale for such modulations is on the order of (Mazeh & Shaham 1979; Paper II)

$$T_{\text{mod}} = P_{AB} \left(\frac{P_{AB}}{P_A} \right) \left(\frac{m_{Aa} + m_{Ab}}{m_B} \right). \quad (9)$$

Thus, for such modulations to be observationally detectable in a relatively short time, one requires a system with a short

outer period, as well as a small outer:inner period ratio. HD 109648 satisfies both these requirements, with an outer period about 120.5 days and a period ratio near 22:1. This results in $T_{\text{mod}} \sim 15$ years, one of the shortest modulation timescales known for a late-type triple system. Our observations of HD 109648 span more than eight years, giving us some hope that we may be able to detect changes in some of the orbital parameters.

3.1 Modulation of the inner eccentricity and the longitudes of periastron

One effect expected from the three-body interaction is a modulation of the inner binary eccentricity (Mazeh & Shaham 1979). The presence of the third star causes a quasi-periodic variation in the inner eccentricity, e_A , around an average value. The amplitude of the eccentricity modulation strongly depends on the eccentricity of the outer orbit (Mazeh & Shaham 1979) and on the relative inclinations between the orbital planes (Mazeh, Krymolowski & Rosenfeld 1997; Paper II), with coplanar situations producing the least effect.

The inner eccentricity modulation goes together with the motions of the lines of apsides of the two orbits (Mazeh, Krymolowski & Rosenfeld 1997; Paper II; Holman, Touma & Tremaine 1997), which manifest themselves through the variation of the longitudes of periastron. Both modulations, that of the inner binary eccentricity and that of the longitudes of periastron can be observed as changes in the elements derived for the two orbital motions.

Mazeh and Shaham (1979) have shown that the inner eccentricity modulation takes place even when the binary orbit starts as circular one. This aspect of the eccentricity modulation is applicable here, because we expect a binary with a period of about 5.5 days to be completely circularized (Zahn 1975; Mathieu and Mazeh 1984), if it were not for the effect of the third star.

3.2 Precession of the nodes

Another expected modulation results from an effect known as the precession of the nodes (Mazeh & Shaham 1976). In the general case of a non-coplanar triple, the inner and outer angular momentum vectors (\mathbf{G}_A and \mathbf{G}_{AB}) precess around their sum, the total angular momentum (\mathbf{G}), which remains fixed. As a result, the angle between \mathbf{G}_A (or \mathbf{G}_{AB}) and any fixed direction in space (other than that coincident with \mathbf{G}), varies periodically with time.

The observer's line of sight is one such fixed direction. The angle between the line of sight and \mathbf{G}_A is precisely the inner inclination angle i_A , since \mathbf{G}_A is perpendicular to the (instantaneous) inner orbital plane. Similarly, the angle between the line of sight and \mathbf{G}_{AB} is the outer inclination angle i_{AB} . As a result of the precession of the orbital planes we expect to see a periodic modulation of the inner and outer inclination angles. In the case of a fixed relative inclination between the two orbits, the time variations of the inclination angles are given by (Mazeh & Shaham 1976)

$$\cos i_A = \cos \alpha \cos \beta_A + \sin \alpha \sin \beta_A \cos[\omega_p(t-t_0)] \quad \text{and (10)}$$

$$\cos i_{AB} = \cos \alpha \cos \beta_{AB} - \sin \alpha \sin \beta_{AB} \cos[\omega_p(t-t_0)], \quad (11)$$

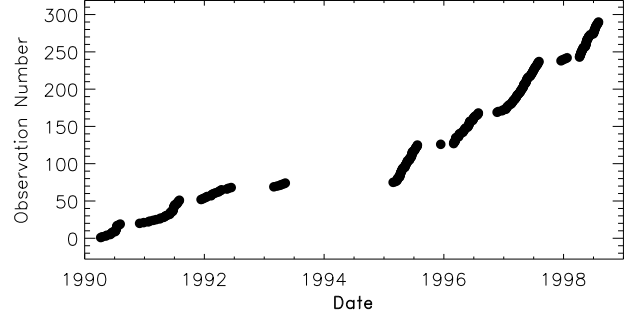


Figure 2. Time history of the 290 observations spanning more than 3000 days.

where α is the angle between the line of sight and \mathbf{G} , β_A is the angle between \mathbf{G}_A and \mathbf{G} , β_{AB} is the angle between \mathbf{G}_{AB} and \mathbf{G} , ω_p is the angular precession frequency and t_0 is a fiducial time determining the phase. An approximate expression for the precession frequency ω_p is given by Mazeh & Shaham (1976); in general it corresponds to the typical modulation timescale given in equation 9. The amplitude of the modulations in the inclination angles are set by α , β_A and β_{AB} , and the variations of i_A and i_{AB} are exactly out of phase.

The modulation of the inclination angles has an immediately observable effect, because the observed amplitudes of the radial velocity variations K in a binary system are directly proportional to $\sin i$ (Mazeh & Shaham 1976; Mazeh and Mayor 1983). Thus, for HD 109648, periodic modulations in the inner inclination angle, i_A , lead to periodic modulations in K_{Aa} and K_{Ab} . Correspondingly, the modulations of i_{AB} would be evidenced by variations in K_A and K_B .

4 SEARCH FOR MODULATIONS INDUCED BY THE THIRD STAR

To search for evidence of modulation of the orbital elements, we have divided our data set and performed orbital solutions on each subset. To obtain a robust orbital solution, we would like as many points in each subset as possible; however, to resolve changes in the elements with time, we would like as many subsets as possible. The ultimate constraint comes from the time history of our observations, shown in Figure 2, which has forced us to use only five subsets. Data from the first few years of observation (before we appreciated the importance of getting good coverage of this system) were combined into one subset, while the observations from each subsequent season form their own subset. We have tried further divisions of the data (e.g., separating the first subset into two), but these provided orbital solutions which were too uncertain to be useful. As expected (Paper II), the inner and outer periods did not vary over the timespan of the observations. Because of this and the fact that our later subsets cover less than two outer periods, in what follows we have fixed the outer period at the value determined by using all the observations.

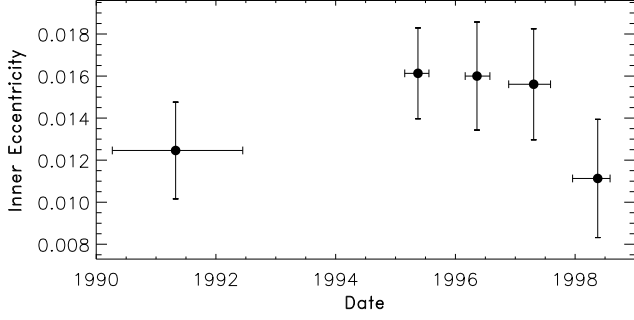


Figure 3. The inner eccentricity as a function of time.

4.1 Modulation of the inner eccentricity and the longitudes of periastron

The inner eccentricity and the longitudes of periastron are presented as a function of time in Figure 3 and Figure 4. In these and subsequent figures, the horizontal “error bars” actually indicate the time span of each subset, while the plotted points are at the mean date within the subset (each observation was given equal weight). There is no obvious modulation of the inner eccentricity, and this fact will enable us to further constrain the geometry of the system in Section 5. However, the fact that inner eccentricity is not zero (as would be expected due to tidal circularization of such a close binary) is evidence for interaction with the third star. More convincingly, the inner and outer longitudes are clearly varying. The roughly linear trend indicates a secular advance of the line of apsides, a direct indication of the effect of three-body interaction.

4.2 Precession of the nodes

The radial velocity amplitudes, K_{Aa} , K_{Ab} , K_A and K_B , from the five subsets are shown in Figure 5. The amplitudes of the inner binary, K_{Aa} and K_{Ab} , both show very clear variation, with the same trend. This is well understood if we assume the variation is caused by the precession of the nodes. To show that this is the case we note the $K_{Aa} = V_{Aa} \sin i_A$, where V is used to denote the true orbital velocity amplitude rather than the projected radial velocity amplitude, and $K_{Ab} = V_{Ab} \sin i_A$. Variation of the inclination angle would thus induce the same trend for K_{Aa} and K_{Ab} .

Furthermore, if the variations of the observed amplitudes are caused only by the modulation of the inclination angle, the ratio K_{Aa}/K_{Ab} should remain constant. To check this point we have plotted in Figure 6 the results from the five subsets in the (K_{Aa}, K_{Ab}) parameter space. If the ratio between the two amplitudes is constant, we expect these five points to fall on a straight line that goes through the origin. The figure shows a beautiful confirmation of this prediction. The variation of the amplitude combined with the results for the inner inclination given in Section 2 imply an approximately 4° decrease in i_A over the span of the observations.

Were this a real effect due to precession of the nodes, we would expect an increase in the outer inclination angle, and correspondingly an increase in K_A and K_B . We can calculate the amplitude of such an effect by linearly approximating the

decrease in the inner radial velocity amplitudes. As above, we know that

$$\frac{\Delta K_{Aa}}{V_{Aa}} = \frac{\Delta K_{Ab}}{V_{Ab}} \quad \text{and} \quad \frac{\Delta K_A}{V_A} = \frac{\Delta K_B}{V_B} \quad (12)$$

The lack of significant eccentricity modulation implies that the relative inclination ϕ has remained nearly constant (because of conservation of the total angular momentum), and validates equations 10 and 11. Using these and differentiating $K = V \sin i$ with respect to time yields

$$\frac{1}{V_{Aa}} \frac{dK_{Aa}}{dt} = \frac{1}{V_{Ab}} \frac{dK_{Ab}}{dt} = \omega_p \cot i_A \sin \alpha \sin \beta_A \sin[\omega_p(t-t_0)] \quad \text{and} \quad (13)$$

$$\frac{1}{V_A} \frac{dK_A}{dt} = \frac{1}{V_B} \frac{dK_B}{dt} = -\omega_p \cot i_{AB} \sin \alpha \sin \beta_{AB} \sin[\omega_p(t-t_0)]. \quad (14)$$

Assuming that this first-derivative (i.e. linear) expansion is sufficient to cover the span of our observations, we can take the ratio of these two equations and determine that

$$\frac{\frac{\Delta K_{Ab}}{V_{Ab}}}{\frac{\Delta K_B}{V_B}} = -\frac{\cot i_A \sin \beta_A}{\cot i_{AB} \sin \beta_{AB}}. \quad (15)$$

Because $\mathbf{G} = \mathbf{G}_A + \mathbf{G}_{AB}$, the law of sines can be applied. For a binary orbit, the amplitude of the angular momentum about the centre-of-mass is

$$L \propto \mu [Ma(1-e^2)]^{1/2} \propto \mu M^{2/3} P^{1/3} (1-e^2)^{1/2}, \quad (16)$$

where μ is the reduced mass and M is the total mass. Thus we have

$$\frac{\sin \beta_A}{\sin \beta_{AB}} = \frac{|\mathbf{G}_{AB}|}{|\mathbf{G}_A|} = \left(\frac{\mu_{AB}}{\mu_A} \right) \left(\frac{M_{AB}}{M_A} \right)^{2/3} \left(\frac{P_{AB}}{P_A} \right)^{1/3} \left(\frac{1-e_{AB}^2}{1-e_A^2} \right)^{1/2} \quad (17)$$

Figure 5 shows that $\Delta K_{Ab} \approx -2.9 \text{ km s}^{-1}$. Combining equations 15 and 17 and inserting the parameters for HD 109648 from Section 2, we expect $\Delta K_B \approx 0.4 \text{ km s}^{-1}$. Our error bars are too large to claim a detection of this, but the expectation is consistent with what we observe. Continued observations may make the precession more clear.

The already observed precession also enables us to strengthen our lower limit on the relative inclination, ϕ_{\min} , calculated in Section 2. Because i_A has been decreasing significantly, while i_{AB} has likely increased slightly, the difference $i_A - i_{AB}$, (which is a strict lower limit on the relative inclination) has also been decreasing. Thus our strongest constraint on ϕ_{\min} can come from analyzing our earliest subset of data only, where $i_A - i_{AB}$ was the greatest, rather than its average value over the whole time span. This yields a refined minimum relative inclination, $\phi_{\min} = 5.4 \pm 0.4^\circ$.

5 SIMULATION

The amplitude of the inner eccentricity modulation is especially sensitive to the relative inclination, ϕ , between the two orbital planes (Mazeh & Shaham 1979; Baily 1987; Paper II). The modulation amplitude increases with the relative inclination. For relative inclinations greater than a critical relative inclination, $\phi \gtrsim \phi_{\text{crit}} \sim 40^\circ$, the modulation amplitude increases dramatically, with the possibility of the inner eccentricity approaching unity. Our observations, spanning more than eight years, have yielded an average inner eccentricity of $e_A = 0.0119 \pm 0.0014$. Using numerical simulations,

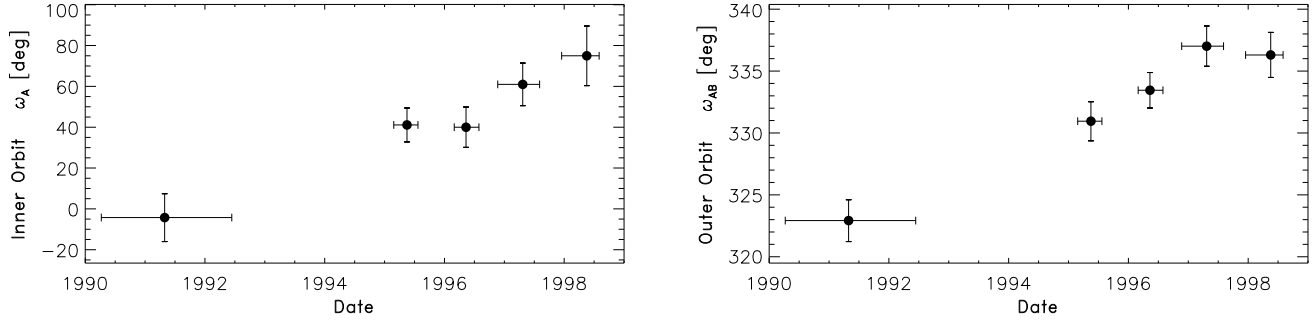


Figure 4. Variation of the inner and outer longitudes of periastron, ω_A and ω_{AB} .

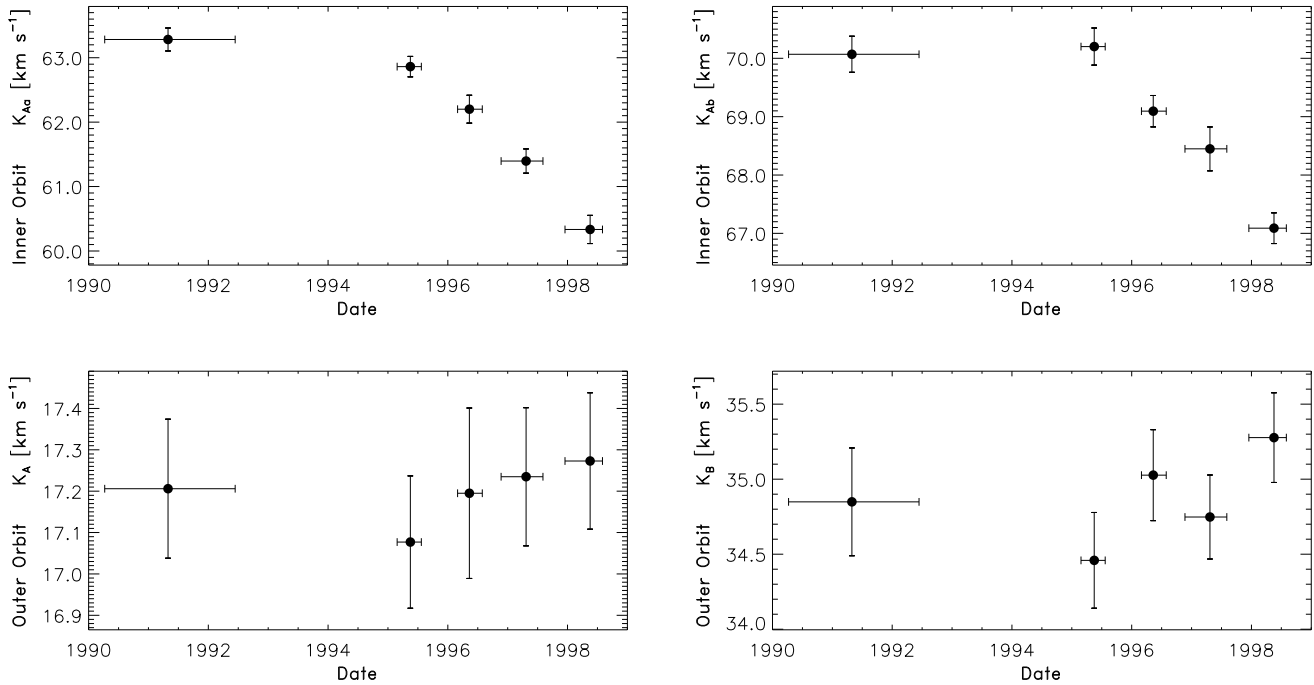


Figure 5. Radial velocity amplitudes. The upper plots show K_{Aa} and K_{Ab} from the inner orbit, while the lower plots show K_A and K_B from the outer orbit. The inner orbit shows clear evidence for the precession of the nodes.

we can estimate the likelihood of this result for different values of the relative inclination angle.

Our simulations are similar to those described in Paper I, integrating Newton's equations for three mass points. The starting point for the integrations was determined from the elements over all the observations, given in Table 2. We have used the three-body regularization program of Aarseth (Aarseth & Zare 1974), as well as a code written by Bailyn (1987), to perform the integrations. We have also developed and used a code written specifically for this system. All three routines yielded identical results.

Typical results of the simulations are shown in Figure 7. As discussed in Paper II, the eccentricity modulation depends not only on the relative inclination, but also on the arguments of periastron, g_A and g_{AB} , measured with respect to the unknown intersection of the orbital planes (Söderhjelm 1984; Paper II). These arguments are especially important at the lower relative inclinations. We have ex-

plored a range of values, so that our simulations are typical cases.

As the figure shows, for small relative inclinations an eight-year window could easily produce an eccentricity modulation consistent with what we have observed. At higher relative inclinations, however, the probability of obtaining a small average inner eccentricity over eight years decreases. By running many different simulations, we can quantify this probability, and estimate an upper limit to the relative inclination, $\phi_{\max} \simeq 54^\circ$ above which a low inner eccentricity cannot be maintained for eight years. However, our simulations were limited, considering only Newtonian gravity with three point masses. Other effects, including quadrupole perturbations in the inner binary, tidal friction and general relativistic effects, may be significant factors in the eccentricity modulation. In particular, such effects may dampen the eccentricity modulation amplitude at high relative inclinations

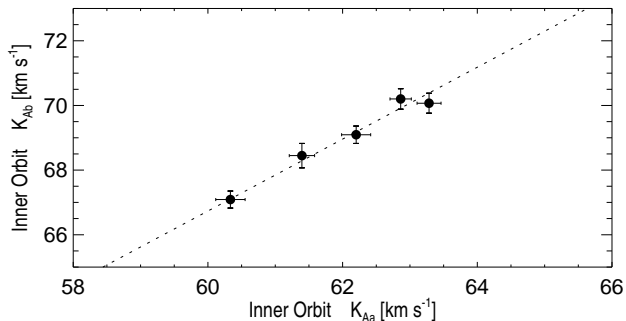


Figure 6. Solutions from the five separate data subsets, plotted in (K_{Aa}, K_{Ab}) space. The dashed line is the best-fit straight line which goes through the origin, expected for constant K_{Aa}/K_{Ab} ratio.

and thus our estimate of the upper limit on the relative inclination is not very firm.

On the other hand, we have a strong lower limit on the relative inclination calculated in Section 2 from the geometry of the system and strengthened in Section 4 via the precession of the nodes. Using this technique, thus, we can significantly constrain the relative inclination. It turns out that the ambiguity in the inclination angles corresponds to an outer orbit which either co-rotates or counter-rotates with respect to the inner orbit. Choosing the inclination angles in the same quadrant corresponds to the co-rotational case, with limits on the relative inclination,

$$5.4^\circ \leq \phi \lesssim 54^\circ \quad (\text{co-rotation}). \quad (18)$$

The counter-rotational case leads to alternative limits for the relative inclination,

$$126^\circ \lesssim \phi \leq 174.6^\circ \quad (\text{counter-rotation}). \quad (19)$$

The relative inclinations closer to ϕ_{\max} (i.e. the upper limit in the co-rotational case or the lower limit in the counter-rotational case) are less probable than those closer to ϕ_{\min} .

6 DISCUSSION

We have shown that HD 109648 is a hierarchical triple system, with an outer period and outer:inner period ratio conducive to modulations of orbital elements on timescales of about a decade. Indeed, our observations clearly indicate an advance of the inner longitude of periastron corresponding roughly to this timescale. We also found strong evidence for variations of the radial velocity amplitudes of the inner orbit, most naturally accounted for by the precession of the nodes. Furthermore, the inner eccentricity is small but significant, presumably due to the interaction with the outer star.

Such effects have been predicted theoretically for hierarchical triples for a number of years. However, there have been few observational confirmations. Mayor and Mazeh (1987) have looked for evidence of the precession of nodes in a number of close binaries, and have reported several significant changes, based on observations made at two widely-spaced epochs. Mazeh and Shaham (1976) also suggested a few sys-

tems where the effect may have had a role, but none of these were confirmed triples.

The inner eccentricity modulation has been less conclusively observed. Mazeh and Shaham (1977; 1979) have postulated it to be the cause of long-period phenomena, such as episodic accretion, in some close binaries. More convincing evidence has been offered for the interaction of a third star with the tidal circularization of the inner binary. Mazeh (1990) has looked for eccentric orbits in samples of short-period binaries that should have been circularized, as a fingerprint for a third star in the system. Three such examples were found, and the hypothesis of a triple system was confirmed in each case. In addition, one system (HD 144515) showed evidence for a variation in the inner eccentricity, again based on observations from two epochs. Ford, Kozinsky, and Rasio (1999) also provide instances of some other triple systems where these interactions may have played a role.

HD 109648 provides the best observational evidence so far of these predicted modulations. This system is a confirmed hierarchical triple, a direct result of analysing the triple-lined spectra. Furthermore, the evidence for variations in the elements comes from observations in a homogeneous set of data, rather than relying on two-epoch observations. Finally, we see evidence both for the precession of the nodes and for the apsidal advance in the same system.

More data are needed to strengthen this case. With better information on the variation of the elements with time, we should be able to derive better constraints on the orientation of the system. For example, if we are able to fit the variation of the inner and outer inclination angles, we can determine the various angles between the total angular momentum and its inner and outer binary components, as well as the angle between the total angular momentum and the line of sight. If the inner eccentricity modulation becomes clearer with additional data as well, it should provide stronger constraints on the relative inclination.

In addition to continued spectroscopic observations, there may be some hope that interferometric observations of HD 109648 will be able to help clarify the orientation of the system. The Hipparcos parallax for HD 109648 of 4 mas may potentially be in error due to the outer orbit, particularly because the outer period is nearly commensurate with one year. Nevertheless, the separation of the third star from the inner binary is on the order of a few mas, allowing for the possibility of a visual orbit in the future.

We can also hope that additional triple systems will be discovered, perhaps ones that are even better than HD 109648 for this type of study. Indeed, Saar, Nördstrom & Andersen (1990) have noted a promising system with a modulation timescale perhaps shorter even than that of HD 109648. Determining the geometry and orientation of such systems will be a great advance in our understanding of them.

ACKNOWLEDGMENTS

We would like to thank J. Caruso and J. Zajac for making many of the observations presented here, as well as R. Davis for help with the data reduction. We are grateful for the efforts of S. Chanmugam, T. Lynn, M. Morgan and E. Scarpicco for their initial work in determining periods for the two

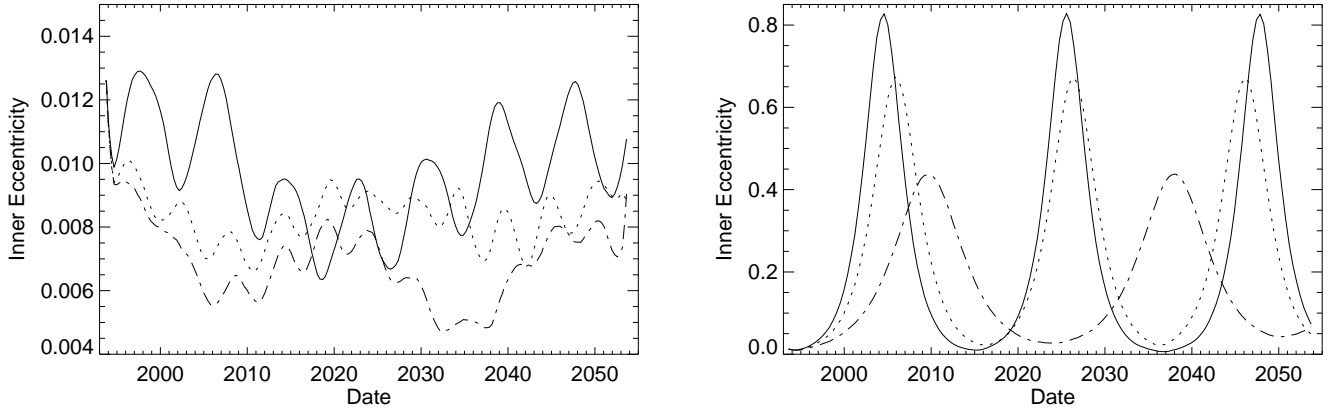


Figure 7. Typical simulation results for the inner eccentricity modulation. The left panel shows the modulation for low relative inclination (dash-dotted: $\phi = 6^\circ$, dotted: $\phi = 15^\circ$, solid: $\phi = 30^\circ$). The modulation shown in the right panel is for high relative inclination (dash-dotted: $\phi = 50^\circ$, dotted: $\phi = 60^\circ$, solid: $\phi = 70^\circ$).

orbits. Thanks also go to S. Aarseth and C. Bailyn for use of their three-body codes. We thank the anonymous referee for providing useful suggestions. This work was supported by US-Israel Binational Science Foundation grant 94-00284 and 97-00460 and an NSF Graduate Research Fellowship. SJ thanks the Harvard University Department of Astronomy for its support of this work. SJ would also express his sincere gratitude to Y. Krymowski for many helpful discussions and his wonderful generosity.

REFERENCES

- Aarseth S. J., Zare K., 1974, *Celest. Mech.*, 10, 185
 Bailyn C. D., 1987, Ph.D. thesis, Harvard University
 Batten A. H., 1973, *Binary and Multiple Systems of Stars*, Pergamon Press, New York
 Baumgardt, H. 1998, *A&A*, 340, 402
 Duquennoy A., Mayor M., 1991, *A&A*, 248, 485
 Fekel F. C., Jr, 1981, *ApJ*, 246, 879
 Ford E. B., Kozinsky B., Rasio F. A., 1999, *ApJ*, in press (astro-ph/9905348)
 Gatewood G., De Jonge J. K., Castelaz M., Han I., Persinger T., Prosser J., Reiland T., Stein J., 1988, *ApJ*, 332, 917
 Gray, D. F., 1992, *The Observation and Analysis of Stellar Photospheres*, Cambridge University Press, Cambridge
 Griffin R. F., 1992, in Duquennoy A., Mayor M., eds, *Binaries as Tracers of Stellar Formation*. Cambridge Univ. Press, Cambridge, p. 96
 Hale, A., 1994, *AJ*, 107, 306
 Holman M., Touma J., Tremaine S., 1997, *Nature*, 386, 254
 Horne J. H., Baliunas S. L., 1986, *ApJ*, 302, 757
 Jha S., Torres G., Stefanik R. P., Latham D. W., 1997, *Baltic Astronomy*, 6, 55
 Krymowski Y., 1995, M.Sc. thesis, Tel Aviv University
 Krymowski Y., Mazeh T., 1998, *MNRAS*, 304, 720 (Paper II)
 Kurucz R. L., 1992, *Proc. IAU Symp.* 149, 225
 Latham D. W., 1985, in Philip A. G. D., Latham D. W., eds, *Stellar Radial Velocities*, IAU Coll. No. 88, L. Davis Press, Schenectady, p. 21
 Latham D. W., Mazeh T., Carney B. W., McCrosky R. E., Stefanik R. P., Davis R. J., 1988, *AJ*, 96, 567
 Latham D. W., 1992, in McAlister H. A., Hartkopf W. I., eds, *Complementary Approaches to Double and Multiple Star Research*, IAU Colloq. 135, ASP Conference Series v. 32, p. 110
 Mathieu, R.D., Mazeh, T., 1988, *ApJ*, 326, 256
 Mathieu R. D., Duquennoy A., Latham D. W., Mayor M., Mazeh T., Mermilliod, J.-C., 1992, in Duquennoy A., Mayor M., eds, *Binaries as Tracers of Stellar Formation*, Cambridge Univ. Press, Cambridge, p. 278
 Mayor M., Mazeh T., 1987, *A&A*, 171, 157
 Mazeh T., 1990, *AJ*, 99, 675
 Mazeh T., Shaham J., 1976, *ApJ*, 208, L147
 Mazeh T., Shaham J., 1977, *ApJ*, 213, L17
 Mazeh T., Shaham J., 1979, *A&A*, 77, 145
 Mazeh T., Krymowski Y., Latham D. W., 1993, *MNRAS*, 263, 775 (Paper I)
 Mazeh T., Krymowski Y., Rosenfeld G., 1997, *ApJ*, 477, L103
 Mazeh, T., Mayor, M., 1983, in *Current Techniques in Double and Multiple Star Research*, I.A.U. Coll. No. 62, eds. R.S. Harrington and O.G. Franz, Publ. of the Lowell Observatory; IX; 120
 Saar S. H., Nördstrom B., Andersen J., 1990, *A&A*, 235, 291
 Scargle J. D., 1982, *ApJ*, 263, 835
 Söderhjelm S., 1984, *A&A*, 141, 232
 Stefanik R. P., Caruso J. R., Torres G., Jha S., Latham D. W., 1997, *Baltic Astronomy*, 6, 137
 Tokovinin A. A., 1997, *A&AS*, 124, 75
 Tokovinin A. A., 1999, *A&AS*, 136, 373
 Upgren A. R., Rubin V. C., 1965, *PASP*, 77, 355
 Upgren A. R., Philip A. G. D., Beavers W. I., 1982, *PASP*, 94, 229
 Zahn, J. P., 1975, *A&A*, 41, 329
 Zucker S., Mazeh T., 1994, *ApJ*, 420, 806
 Zucker S., Torres G., Mazeh T., 1995, *ApJ*, 452, 863

APPENDIX A: RADIAL VELOCITIES

In the following table we list our observations of the heliocentric radial velocities for the three visible components of HD109648. The date given is HJD - 2400000, and the velocities are in km s^{-1} .

Table A1. HD109648 radial velocities

Date	v_{Aa}	v_{Ab}	v_B
47989.7237	8.27	-71.69	3.49
47999.7229	-61.78	-0.48	5.75
48020.6318	-91.61	38.78	5.81
48026.5976	-81.05	35.39	-5.62
48047.6212	-56.23	58.64	-55.31
48050.6484	62.67	-70.83	-54.71
48058.5622	-53.61	62.15	-59.52
48059.5741	-50.88	56.89	-56.80
48078.5968	43.71	-75.39	-33.52
48079.5639	-14.67	-14.66	-31.02
48082.5545	2.21	-32.98	-20.68
48083.5582	46.24	-86.64	-23.75
48084.5680	13.92	-49.12	-21.77
48086.5908	-81.22	47.77	-20.62
48087.5809	-36.27	-3.84	-23.73
48088.5697	30.87	-77.91	-17.47
48089.5811	34.05	-83.29	-16.95
48102.5641	-88.51	38.11	-3.03
48108.5458	-90.10	38.41	-0.47
48226.8598	11.62	-73.25	1.26
48251.9081	-47.72	-11.73	10.72
48279.9641	17.77	-52.29	-32.17
48288.8245	-61.96	63.08	-52.66
48309.7793	-15.70	3.53	-46.37
48327.8502	-75.92	43.35	-19.55
48349.7883	-86.76	32.36	1.96
48354.7527	-94.22	38.24	5.32
48372.6173	-35.18	-30.36	10.47
48380.6620	-16.25	-42.88	6.52
48385.6606	15.24	-77.57	-2.72
48395.6641	40.76	-84.38	-19.89
48409.6348	-61.88	65.74	-57.33
48413.6430	7.05	-5.73	-58.60
48414.6856	-53.57	61.53	-58.13
48415.6193	-50.53	61.78	-58.18
48428.5738	57.32	-73.48	-49.80
48429.5644	35.66	-52.56	-47.59
48431.5744	-67.68	57.96	-46.16
48432.5571	-31.54	24.11	-43.70
48433.5852	36.34	-56.62	-39.55
48434.5791	52.37	-75.33	-41.49
48435.5893	-4.54	-15.46	-35.88
48438.5786	-1.85	-26.92	-34.98
48439.5541	48.44	-81.45	-27.24
48442.5782	-76.91	52.03	-26.14
48454.5700	-41.14	-3.22	-11.80
48456.5764	34.51	-88.69	-14.46
48458.5707	-82.10	39.30	-7.50
48462.5412	9.60	-64.66	-4.10
48466.5641	19.99	-81.09	-0.80
48469.5647	-86.54	33.22	1.36
48601.9412	-82.25	26.99	9.14
48612.8884	-83.48	24.34	9.55
48621.9574	-34.13	-24.48	3.54
48632.8870	-24.36	-24.90	-9.53
48638.8574	-51.46	22.95	-23.83
48662.8834	-10.31	11.97	-58.74
48665.8606	-10.21	9.42	-56.13
48669.9563	59.43	-74.15	-50.67
48679.7531	7.64	-36.26	-33.01
48691.7352	44.20	-91.01	-14.88

Table A1 – *continued*

Date	v_{Aa}	v_{Ab}	v_B
48706.7376	-35.67	-15.70	0.75
48711.7672	-66.89	13.10	2.95
48721.6201	-93.70	34.41	10.33
48726.6840	-78.76	16.65	7.98
48759.6447	-65.65	36.28	-25.29
48768.6163	58.58	-74.76	-47.66
48785.6718	40.20	-45.64	-58.69
49045.8374	-60.86	34.77	-27.26
49065.8097	-38.38	-17.99	-3.76
49082.7215	-72.76	13.25	7.67
49092.6583	-5.49	-61.83	4.93
49106.6988	-34.95	-24.62	1.48
49115.7127	-69.84	28.48	-12.82
49773.7397	-80.37	50.52	-19.63
49786.8017	17.02	-77.36	-5.51
49795.7514	-90.82	41.62	2.87
49796.7069	-53.68	-2.26	3.79
49799.7128	-26.93	-32.54	5.53
49801.8641	-73.75	18.64	8.16
49802.7256	-17.64	-47.75	6.78
49812.7374	-79.52	19.43	10.31
49813.6946	-18.40	-49.16	9.11
49814.8387	30.79	-102.61	8.91
49815.7253	0.69	-69.38	7.59
49817.7980	-92.81	34.62	8.20
49818.6922	-51.15	-9.88	9.38
49819.7020	14.21	-86.23	7.75
49822.7849	-91.01	35.77	7.31
49824.6775	-13.81	-48.19	5.84
49825.8203	33.53	-101.22	5.07
49828.6516	-90.42	39.92	3.55
49831.6661	30.23	-91.54	0.11
49832.6810	-28.65	-23.83	-2.44
49844.6766	-74.82	49.36	-25.82
49845.6847	-57.39	31.17	-25.54
49846.6568	7.51	-36.18	-30.87
49847.6814	52.54	-82.92	-31.62
49851.6380	-20.41	5.17	-42.99
49854.6451	-11.74	0.60	-48.20
49857.6233	21.91	-26.35	-52.17
49858.6378	63.86	-70.39	-54.37
49860.6530	-41.31	45.52	-59.99
49861.5812	-60.33	73.00	-58.02
49873.5634	-16.18	13.82	-50.70
49874.6595	50.08	-64.86	-51.72
49875.6122	50.61	-64.67	-48.90
49876.5639	-10.27	3.28	-48.88
49884.6025	-19.25	-2.15	-33.72
49885.6143	42.48	-70.01	-31.00
49886.5958	40.49	-69.83	-29.20
49887.5696	-23.48	-1.81	-25.58
49888.5820	-73.23	53.88	-27.01
49889.5828	-54.25	30.32	-23.22
49890.6078	12.64	-47.17	-22.63
49891.5853	47.28	-85.71	-20.76
49901.5663	5.02	-53.63	-9.04
49903.5623	-1.71	-47.24	-6.70
49905.5629	-82.56	39.32	-5.78

Table A1 – *continued*

Date	v_{Aa}	v_{Ab}	v_B
49909.5579	-42.72	-11.48	-3.03
49911.5591	-63.54	15.05	1.49
49913.6108	34.38	-97.08	3.70
49918.5850	27.62	-94.18	4.70
49920.5635	-50.20	-8.34	8.08
49921.5781	-92.65	36.67	7.68
50063.9522	-91.42	36.99	7.72
50142.7836	14.33	-66.60	-9.83
50143.8448	35.45	-90.43	-8.06
50146.7695	-78.21	33.86	-3.59
50151.8049	-90.40	39.96	-1.16
50152.8799	-46.78	-6.37	0.80
50153.7820	12.21	-74.33	3.74
50154.8156	29.80	-95.35	1.76
50155.8299	-26.69	-30.71	2.78
50156.6971	-80.02	26.01	3.80
50172.7725	-64.97	4.87	7.90
50173.8092	-93.74	34.74	9.02
50174.8187	-48.98	-12.96	9.56
50176.8073	24.37	-96.12	8.06
50177.7284	-30.72	-33.34	7.19
50185.7026	-51.35	-6.47	5.49
50198.5911	35.74	-90.65	-8.14
50201.6261	-69.71	33.64	-14.13
50202.6803	-3.42	-37.85	-15.35
50206.6064	-76.90	52.93	-25.11
50210.6036	-9.49	-10.95	-35.23
50211.7135	-67.17	56.52	-39.18
50216.6774	-40.16	38.35	-48.67
50228.7005	-57.98	68.09	-60.26
50229.5814	-17.83	21.07	-61.32
50233.5826	-58.14	62.18	-53.43
50235.6004	16.07	-21.89	-51.92
50236.6059	59.03	-69.41	-50.02
50237.6100	27.84	-37.62	-49.40
50239.6119	-65.37	62.10	-44.99
50240.6300	-19.83	8.50	-45.50
50242.5957	47.45	-69.39	-40.01
50258.5729	42.22	-89.86	-15.70
50260.5793	-61.65	21.44	-12.95
50261.5914	-81.30	42.94	-11.88
50263.5636	26.28	-79.50	-9.25
50266.6003	-85.36	42.25	-6.34
50270.5630	1.03	-55.75	-2.40
50275.5685	22.59	-84.41	1.81
50285.5636	23.13	-92.08	7.40
50287.5558	-45.50	-14.82	9.06
50292.5516	-11.93	-55.50	11.11
50293.5451	-77.62	19.16	10.68
50407.9227	-31.85	-31.77	7.18
50415.9494	-43.78	-20.20	10.36
50437.9290	-29.53	-11.90	-5.62
50443.9209	6.92	-52.32	-18.57
50460.9211	54.87	-62.26	-57.42
50462.9635	-20.03	21.95	-58.43
50465.8867	32.72	-30.65	-60.69
50467.9641	15.05	-14.34	-62.34

Table A1 – *continued*

Date	v_{Aa}	v_{Ab}	v_B
50472.9241	45.63	-54.75	-56.50
50477.8895	56.86	-69.28	-51.02
50481.9188	-5.94	-6.37	-44.48
50492.8095	-19.26	-15.75	-22.29
50495.8587	-39.35	7.02	-18.69
50499.8407	40.18	-90.05	-14.82
50502.8649	-74.78	36.56	-10.20
50504.8512	33.71	-93.86	-9.28
50507.8283	-85.63	42.91	-3.88
50514.8631	-19.30	-38.91	5.08
50516.8764	11.82	-71.16	0.87
50521.7889	28.84	-98.68	3.24
50523.7647	-83.61	21.19	2.86
50526.6975	24.94	-92.82	6.81
50528.8336	-61.17	2.61	6.38
50530.8489	-54.04	-7.41	8.86
50535.6834	-87.28	28.47	9.36
50540.7280	-93.20	35.94	7.23
50543.7510	27.71	-98.32	7.76
50548.7202	29.56	-94.34	2.31
50550.7073	-56.17	-1.10	5.47
50552.7438	-49.91	-7.01	1.65
50554.6823	32.37	-93.86	-1.04
50559.7188	35.81	-91.00	-8.35
50561.6376	-47.89	5.79	-13.11
50565.6876	39.91	-81.27	-20.57
50567.6871	-71.29	49.65	-22.03
50569.6653	-2.94	-27.34	-27.64
50569.7151	-0.35	-27.81	-28.61
50571.6093	29.76	-56.43	-32.20
50573.5884	-69.39	58.27	-39.81
50581.6726	60.56	-66.47	-55.04
50583.6745	-32.28	37.28	-59.00
50584.5720	-59.02	70.28	-60.46
50586.6867	46.14	-46.93	-61.62
50587.5819	62.05	-64.78	-61.81
50589.5764	-50.38	62.36	-60.94
50591.6532	15.57	-15.47	-61.18
50595.6468	-60.57	67.52	-57.21
50597.5898	39.31	-55.07	-48.82
50608.5644	31.64	-56.79	-31.49
50610.5844	-13.25	-13.34	-29.83
50614.5538	42.61	-82.71	-22.75
50616.6050	-53.81	21.35	-19.12
50619.5932	26.68	-70.98	-14.71
50622.6245	-80.05	40.79	-12.74
50624.6218	-1.81	-48.60	-10.44
50627.5643	-61.05	13.59	-6.69
50629.5753	-41.50	-10.38	-2.73
50631.6240	24.56	-87.12	-0.82
50634.5747	-71.58	14.22	-1.88
50636.5764	32.29	-97.93	2.85
50640.5665	-41.46	-15.53	4.26
50642.5644	21.57	-90.07	4.42
50646.5856	-8.72	-58.15	5.18
50649.5672	-74.46	12.44	6.12
50653.5645	19.97	-90.01	8.11
50655.5699	-91.39	32.95	8.40
50656.5551	-72.95	14.22	5.63
50660.5468	-74.84	15.02	1.76
50663.5513	21.44	-89.77	8.56

Table A1 – continued

Date	v_{Aa}	v_{Ab}	v_B
50797.9062	-83.63	37.29	-5.48
50803.8913	-79.47	43.31	-12.35
50814.9400	-66.79	53.63	-41.84
50825.9076	-55.69	64.16	-60.69
50834.9095	22.09	-23.55	-58.83
50910.6468	29.72	-96.99	4.00
50911.6455	-11.34	-49.39	2.67
50914.6172	-29.06	-27.43	0.81
50915.6724	26.84	-90.62	0.58
50917.7045	-48.18	0.08	-3.80
50918.7243	-86.02	40.70	-3.73
50919.7225	-51.31	4.70	-4.78
50922.6137	-5.00	-43.91	-11.45
50924.6904	-71.70	36.36	-14.91
50925.6614	-17.19	-19.51	-15.24
50929.6813	-76.37	51.08	-25.92
50931.6316	21.59	-51.75	-30.75
50932.6945	44.88	-76.60	-32.51
50934.6477	-59.04	46.01	-37.73
50945.7289	-49.81	62.03	-58.25
50946.7063	-46.23	55.96	-59.89
50948.6479	59.44	-64.30	-59.96
50949.6324	42.59	-44.57	-60.96
50950.6296	-22.94	29.47	-63.94
50951.7112	-61.31	68.11	-57.60
50952.7105	-18.26	23.38	-60.51
50953.5900	36.55	-37.49	-61.43
50954.6430	58.71	-64.29	-58.83
50956.5913	-50.20	54.90	-55.59
50958.6129	5.79	-10.27	-52.67
50961.6626	-33.40	27.84	-49.03
50964.5528	28.95	-49.47	-42.92
50966.5663	1.02	-21.17	-39.88
50968.5815	-60.31	44.96	-33.71
50974.5877	-39.63	7.86	-28.00
50976.5979	40.66	-80.78	-20.83
50993.5849	6.59	-66.82	0.10
50996.6379	-41.89	-12.75	0.72
50997.5898	14.54	-79.85	-0.51
50998.5910	25.37	-91.13	3.73
51000.5831	-86.95	27.19	4.43
51000.6085	-86.04	31.18	2.89
51004.5778	0.20	-64.65	4.94
51005.5690	-65.26	7.19	3.71
51006.5708	-90.43	34.43	5.64
51008.5673	15.48	-83.70	10.36
51009.5967	25.15	-90.61	13.22
51013.5759	-12.46	-54.37	9.80
51014.5698	26.17	-99.64	7.41
51019.5842	15.79	-87.62	9.55
51020.5530	21.55	-92.12	8.06
51024.5518	-11.33	-56.40	7.86
51026.5814	-5.79	-60.56	5.04